

High temperature superconductors at optimal doping

W E Pickett

Department of Physics, University of California, Davis, California, 95616

(Received 20 March 2006; accepted 12 May 2006)

Abstract

Intensive study of the high temperature superconductors has been ongoing for two decades. A great deal of this effort has been devoted to the underdoped regime, where the new and difficult physics of the doped Mott insulator has met extra complications including *bilayer coupling/splitting*, *shadow bands*, and *hot spots*. While these complications continue to unfold, in this short overview the focus is moved to the region of actual high- T_c , that of optimal doping. The focus here also is not on the superconducting state itself, but primarily on the characteristics of the normal state from which the superconducting instability arises, and even these can be given only a broad-brush description. A reminder is given of two issues: (i) why the “optimal T_c ” varies: for n -layered systems it increases for n up to 3, then decreases; for a given n , T_c increases according to the ‘basis’ atom in the order Bi, Tl, Hg; (ii) how does pressure, or a particular uniaxial strain, increase T_c when the zero-strain system is already optimally doped?

Keywords: high temperature superconductors, optimal doping, Mott insulator

1. Introduction

For two decades the cuprate high temperature superconductors (HTS) have provided excitement, entirely new areas of the materials behavior to be explored (beside the superconductivity), and fertile ground for broad intellectual speculation on what the underlying microscopic processes are, and even more generally what else might be possible and simply not observed yet. This broad area continues to drive numerous workshops and conferences each year, and to continue research funds being allocated into this and closely related areas.

The initial question was of course “what can the mechanism be?” but the complexity of the materials has always led the accumulated understanding, so this query has not been answered to hardly anyone’s satisfaction. In an attempt to build a consistent overall picture, mapping out and forming a rudimentary understanding of the temperature-doping phase diagram became a primary focus of research. In this pursuit, a great deal has been accomplished, with the most effort being expended on $\text{YBa}_2\text{Cu}_3\text{O}_{7-\delta}$ (YBCO), $\text{Bi}_2\text{SrCa}_2\text{Cu}_2\text{O}_{8+\delta}$ (BSCCO, or more specifically Bi2212), and $\text{La}_{2-x}\text{Sr}_x\text{CuO}_4$ (LSCO). There are noticeable differences in some aspects of behavior between the various families, but the similarities in many aspects of their behavior are clear.

The mapping of the phase diagram has employed the full spectrum of experimental probes: transport

(resistivity, thermopower, and Hall data have all been important), thermodynamics (susceptibility and heat capacity are two of the most basic probes), spectroscopy (NMR and NQR, tunneling and scanning tunneling microscopy, neutron scattering, IR \leftrightarrow UV conductivity, ARPES, XPS probes) – all have played their part. On the theoretical side, the questions posed by HTS have provided an enormous spurt in new concepts and approaches, numerical algorithms, and stimulating results as all types of theorists have played their part in adding to understanding the difficult data.

In this brief overview the “big picture” will be pushed aside to focus more directly on the region of optimal doping: what are the phenomena observed when the system is at its peak T_c ? From this vantage point, superconductivity begins to be destroyed both by decreased doping, with its encroachment of strong charge and AFM magnetic fluctuations, and by increased doping with its return to a conventional metallic state. It worth noting that *optimal doping* in the usual sense does not mean *optimal T_c* ; for example, pressure or uniaxial strain can increase T_c even beginning at optimal doping. The purpose here is simply to inform or remind, from a somewhat uncommon viewpoint at the “peak”.

2. Phase diagram

There is some level of consensus on the main features of the temperature-doping phase diagram, shown schematically in figure 1. At the low/zero-doping side is

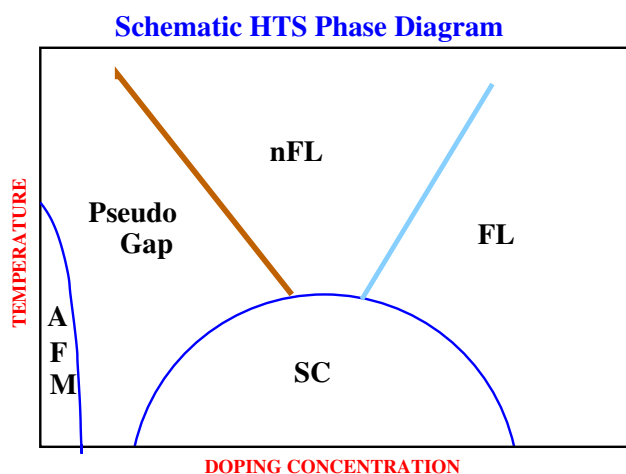


Figure 1. (color online) Schematic temperature-doping phase diagram for the class of layered copper oxide superconductors. The phases, discussed more fully in the text, are antiferromagnetic (AFM) for very small doping concentration, a weakly metallic PseudoGap phase, a metallic but peculiar non-Fermi liquid (nFL) phase, a metallic Fermi liquid (FL) phase in the overdoped regime, and the superconducting (SC) state.

the Mott insulating antiferromagnetic (AFM) phase; at the high-doping side is a rather conventional Fermi liquid (FL) metal where the magnetic fluctuations become weak and interaction-induced enhancement of thermodynamic properties can be accounted for in the standard manner. Above T_c there is a roughly fan-shaped regime characterized as a peculiar metal, a non-Fermi liquid phase. The region that has been studied extensively in the past fifteen years is the weakly-metallic pseudogap phase where spectral weight is displaced from the lowest energy region (leading to the characterization as ‘pseudogap’). There has been speculation that there is a quantum critical point at $T=0$ around optimal doping, where the PseudoGap-nFL and nFL-FL phase boundaries might meet if extrapolated into the SC regime. Support for this generic phase diagram can be found, for example, in the presentations of Timusk and Statt[1] and of Ando *et al.*[2] to mention only two of many papers on the subject.

The HTS phase diagram is interesting indeed. It seems however that it is not only not unique to HTS, but that this general sort of phase diagram may be common to several other classes of superconductors. A similar phase diagram for the organic superconductor class κ -(BEDT-TTF)₂X, X = Cu[N(CN)₂]Cl, Cu[N(CN)₂]Br, or Cu(NCS)₂, presented by McKenzie[3], with maximum T_c an order of magnitude lower, is shown in figure 2. No pseudogap phase is identified in the organic superconductors, but the AFM \leftrightarrow nFL \leftrightarrow FL regimes surrounding the SC phase are quite similar.

The heavy fermion superconductors, with maximum T_c yet another order of magnitude lower, also show phase diagrams with considerable similarities, although the phase diagrams for various of the systems differ in their details. However, several systems have, either in the pressure-temperature plane or in the doping-

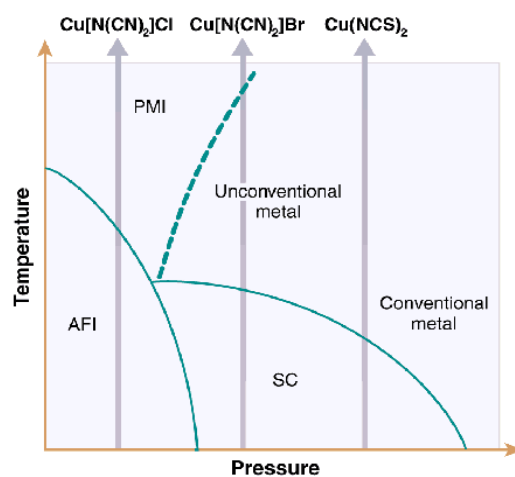


Figure 2. (color online) Schematic temperature-pressure phase diagram of the class of 2D BEDT organic superconductors, as presented by McKenzie[3]. In this system the role of pressure can be played by the choice of the Cu-based counteranion.

temperature plane, a superconducting phase with magnetic order the left, a Fermi liquid (enhanced) to the right, and a nFL phase above T_c . A possible conclusion is that the HTS phase diagram in figure 1 is not really so unusual, but merely one example of a broader class of phase diagrams with many similarities, and a quantum critical point at the base of the superconducting phase. One might even claim that the only thing unique to the HTS is their high superconducting transition temperatures.

3. T_c and optimal doping

The accepted highest T_c produced so far in the cuprates (or anywhere, for that matter) is in HgBa₂Ca₂Cu₃O_{8+ δ} (so-called Hg1223). The value of oxygen excess δ is not very well established, but the ambient $T_c = 134$ K suggests optimal doping. With a pressure of $P_{opt} = 31$ GPa the value $T_c^{max} = 164$ K was achieved by Chu’s group and others[4-7] in 1993. The sister compound Hg1212, having one less CuO₂ layer, reached $T_c = 154$ K at 29 GPa.

The effect of the number of CuO₂ layers has been discussed by many groups, and speculations about why the trend is as it is are many but unconvincing. The primary multi-CuO₂-layer families are Bi-based, Tl-based, and Hg-based, and the maximum value of T_c for a given number of CuO₂ layers increases in that order (Bi; Tl; Hg); there may not even be any serious speculations on the origin of this difference. In these classes, the optimum (with respect to doping) T_c increases up to three layers, then decreases (the four, five... layer compounds get successively harder to synthesize). The question of why three layers is optimal has been asked many times, without any degree of consensus.

4. Inhomogeneity

The topic of inhomogeneity has always been present in HTS systems. Initially it was simply due to (i) the

oxygen non-stoichiometry necessary to dope the materials, and to (ii) the difficulty in producing homogeneous samples even on a several-nanometer scale. However, during the 1990s it gradually became clear that the underdoped HTS materials displayed intrinsic inhomogeneities, as holes are doped into the Mott insulator. Several causes have been pursued extensively: correlated behavior due to strong repulsion (Hubbard U) on the Cu ion; longer range, weakly screened Coulomb interaction between the doped holes; polaronic character (strong electron-lattice coupling) of the carriers and their interactions.

Experimental evidence of organized patterns of inhomogeneity began appearing toward the mid-1990s [8-11]. Terminology including phase separation, polaronic lattices, stripes, and later checkerboard patterns, are among the concepts (originally) and observations (subsequently) that are heavily discussed. Theoretical indications of strong tendencies toward inhomogeneity in doped insulators had begun to appear somewhat earlier [12-15]. Some cases of inhomogeneity are material specific, such as the discovery of a $(1/4,0,0)$ superstructure (four unit cells) in near optimally doped, detwinned crystals of $\text{YBa}_2\text{Cu}_3\text{O}_{6.92}$ [16]. This superstructure may arise from ordering of oxygen vacancies in the chain, and is present in only part of the sample.

Research into the interplay between inhomogeneity and superconductivity has blossomed, and several groups have models of high temperature superconductivity that require, or only occur jointly with, strong inhomogeneity. It has been shown that there are substantial regions in the phase diagram of the 2D negative- U Hubbard model where superconductivity is enhanced by an inhomogeneous pairing mechanism, relative to the same total pairing strength spread homogeneously [17,18].

Scanning tunneling spectroscopy has been developed to a new stage, where it is standard now to display in full color a “gap map” of the surface of a HTS; see the recent study of BSCCO by McElroy *et al.* [19] and references therein. Multiscale inhomogeneity of numerous surfaces has been studied with this method. However, a different and very telling viewpoint arises from the report by the Geneva group of Fischer [20]. They reported scanning tunneling spectroscopy (STS) of high quality $\text{Bi}_2\text{Sr}_2\text{Ca}_2\text{Cu}_3\text{O}_{10+\delta}$ (Bi2223) crystals. In a sample with $T_c = 109$ K, $\Delta T_c = 1$ K (*i.e.* a sharp onset), the STS spectrum is absolutely unvarying over at least 500 Å. Thus the sample is extremely homogeneous. Dose this qualifies as a *smoking gun* indicating that inhomogeneity is neither intrinsic to nor necessary for HTS superconductivity? More study of the degree of inhomogeneity that is present in other optimally doped cuprates is needed. A high precision neutron diffraction study of optimally doped LSCO ($x=0.15$) by Braden *et al.* [21] detected no disorder beyond what could be accounted for by normal thermal vibrations, strongly implying (but not absolutely proving) a lack of electronic

inhomogeneity in this material. Since inhomogeneity seems neither intrinsic nor necessary, a central question then becomes: how is it that the superconducting condensate is so insensitive to the inhomogeneity that is often present. The short coherence length would seem to be a necessity; whether that is sufficient is a question for the experts in that area of study.

5. Selected phenomena at optimal doping

In this section a few observations will be made based on a selection of cuprate characteristics (classes of experiments), each of which has been the focus of a considerable amount of study. Primarily photoemission results are discussed in the first three subsections; more detail and references can be found in two recent reviews [22,23].

5.1. Fermi surfaces; low energy dispersion

It is now widely agreed that the Fermi surface that is observed, and nowadays usually mapped out in considerable detail, agrees with that given by local density approximation (LDA) calculations, *i.e.* by methods that neglect the correlation effects that are very large in the undoped and underdoped CuO_2 layers. Arriving at this consensus was not easy, and the evidence only began to emerge around 1992 for YBCO [24]. More recent evidence will be mentioned below. Indeed for the first 2-3 years after the discovery of HTS, a widely circulated viewpoint was there was no identifiable Fermi surface in these doped Mott insulators. The manner in which the metallic electronic structure asserts itself in a doped Mott insulator is still the focus of a great deal of experimental work and theoretical grappling, which still is saddled with simplified models because of the complexity of the physics. The lack of correlation effects on the Fermi surface at optimal doping can be put in a more pointed way: not only is the LDA Fermi surface observed, but in calculating this Fermi surface the carriers that do the doping can be just “dumped” into the CuO_2 layers treated in LDA.

It is significant also that there is not a single “HTS Fermi surface.” In fact, the Fermi surface shape is material-dependent, even within the hole-doped HTS materials. LSCO is very different from both YBCO and BSCCO with their barrel Fermi surfaces, and both YBCO and BSCCO have their own peculiarities as noted below. The following subsections give a brief discussion of these three most studied HTS classes.

5.2. ARPES spectrum

The evolution of information obtained from photoemission—through the understanding of surface characteristics, and through improvement in momentum and energy resolution and extensions in theoretical analysis - this would be the subject of a *very* long review article in itself. Angle-resolved photoelectron emission spectroscopy (ARPES) is a crucial probe, because it allows a direct probe of the single-particle-like excitations of a metal or superconductor (modulo atom-

specific and energy-dependent matrix elements and photoexcited electron escape depth issues, which can become important). In addition, it can be carried out in both the normal and superconducting states. Much of the recent work has been focused on the underdoped, and occasionally undoped, materials due to their very complex, correlated nature. Recent reviews include those of the Stanford [22] and Argonne National Laboratory[23] groups. In this section the objective is simply to try to characterize briefly the general findings on HTS materials near or at optimal doping.

5.2.1. LSCO

At first sight it seems that LSCO is the simplest, structurally and perhaps also electronically, of the most commonly studied families. However, around $x \approx 1/8$ in the Ba analog (LBCO) there is a lattice instability even when correlations are neglected, *i.e.* predicted from LDA calculations [25] and observed. This lowering of symmetry from tetragonal to orthorhombic also changes the LDA Fermi surface [26] and reduces T_c precipitously. However, the optimally doped region of interest here occurs around $x=0.16$. There is also the question of the effect of the La^{3+} - Sr^{2+} potential disorder on the excitations. The (usually implicit) assumption is that this disorder leads to minor broadening that can be neglected.

A distinctive feature of LSCO is that the Fermi surfaces arising from the cuprate layer has a different orientation from that of the other two most studied systems, YBCO and BSCCO. In fact, the Fermi surface of LSCO is much like that of the 2D nearest-neighbor dispersion used in many Hubbard model studies, while those of YBCO and BSCCO are not. This feature is evident in figure 3, which shows the calculated (LDA) Fermi surface cross-section superimposed on the ARPES data, for slightly overdoped $x=0.20$. Features identified near optimal doping are:

- (i) the Fermi surface consists of the characteristic diamond-type orientation of a square with rounded corners and bowed edges [27].
- (ii) the $(\pi,0)$ and $(0,\pi)$ points are *hot spots*, that is, very low dispersion regions around van Hove singularities [27].
- (iii) somewhat above optimal doping, the topology of the Fermi surface changes [28] from hole-like surfaces centered around (π,π) to electron-like surfaces centered around $(0,0)$, corresponding to the Fermi level moving from above to below the van Hove saddle point. This change of Fermi surface shape, and in sign of the carriers is also seen in LDA band structures and calculated Hall coefficients [29,30].

5.2.2. BSCCO

The micaceous nature of BSCCO allows the easy preparation of clean surfaces *in situ*. Nothing else about BSCCO is simple, however. First, LDA calculations indicate that a Bi-O band may drop below the Fermi level and give rise to a Fermi surface that crosses, and

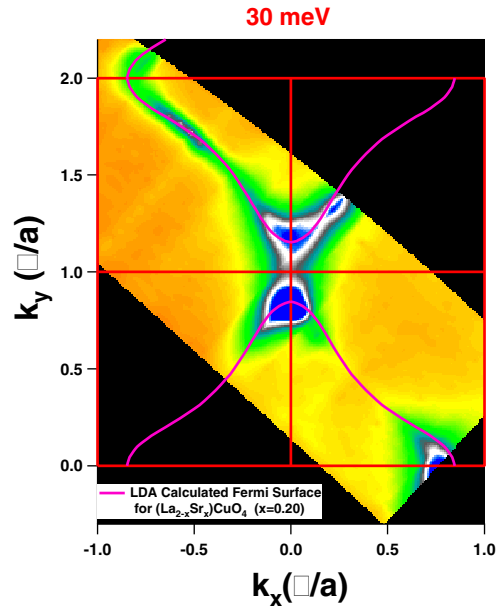


Figure 3. (color online) Calculated Fermi surface of LSCO [26] superimposed on the ARPES data. The long green area illustrates the agreement in shape. The dark blue regions mark the van Hove singularity *hot spots*, which at this concentration nearly, but not quite, touch at the $(0,\pi)$ point.

couples to, the CuO_2 -derived Fermi surfaces that are of most interest [31]. Such calculations must adopt a simplified model of the Bi-O layers, however, because there is a long wavelength superstructure with periodicity $\sim 4.7(a,a,0)$ that shows up very strongly in diffraction data, and also is observed in ARPES data. This superstructure is understood in terms of a misfit between the preferred lattice constants of the Bi-O layers compared to that of the CuO_2 layers. The difficulties in interpreting the data include:

- (i) *shadow bands*, main CuO_2 Fermi surface replicas shifted by (π,π) in the 2D zone [32],
- (ii) *umclapp bands*, originating from the superstructure mentioned above, which produces a zone-folding-like effect [33],
- (iii) *bilayer splitting*, present presumably in all two-layer cuprates and arising from even and odd (bonding, antibonding) combinations of states on the two cuprate layers.

These features continue to make the very complex ARPES data challenging to interpret. Nevertheless, it is accepted that the more persistent parts of the CuO_2 barrel Fermi surfaces are where predicted by LDA calculations. The review of Damascelli *et al.* [22] can be consulted for more details.

5.2.3. YBCO

By 1992 it had become clear [24] from ARPES and positron annihilation spectroscopy that the two CuO_2 layer barrel Fermi surfaces and the CuO chain-derived planar Fermi surface were like those calculated for optimally doped YBCO. The ARPES work to this point

had to cope with surface quality issues (oxygen left the surface even after cleaving *in situ* unless the temperature was kept very low). Further work has had to contend (i) with effects of strong emission from a surface state very near the Fermi level [34] that complicates interpretation, (ii) with the increasing realization that interlayer hopping (k_z dispersion) must be taken into account, as well as the bilayer splitting, [35,36] and (iii) with effects of the Cu-O chain, which contributes a chain-derived band and makes de-twinning necessary. For these reasons ARPES studies of YBCO have become much fewer in the past decade.

Some important progress has been reported, due to sample quality improvement along with the increased resolution that has been essential for spectroscopy of the superconducting state. Lu and collaborators carried out a considerable mapping [37] of the near-Fermi-surface states, and in addition to the obtaining the position in the zone of the surface state, managed to clarify the shape of the CuO₂ layer barrel surfaces and to identify the Cu-O chain band crossing. These features are fully consistent with LDA calculations [24].

5.3. Kinky dispersion

While it should be left to experts to consider just when a bend in the HTS hole dispersion began to be evident, the *kink* observed in ARPES in the 50-70 meV range (varying with material and doping) was strongly emphasized by Bogdanov *et al.* [38] and Lanzara and collaborators [39]. This feature has been verified several times, with considerable effort being expended in trying to shed light on its interpretation and its origin. The consensus is that it arises from interaction with a bosonic excitation in the same energy range, with spin fluctuations and phonons both being strong contenders. Again, we emphasize that the focus in this article is on what is observed in the optimally doped regime. In ferretting out the microscopic origin, the evolution of the feature through the underdoped regime will be of great importance.

It should be recognized that the occurrence of a kink observed in ARPES is not unique to HTS. In 2H-TaSe₂ a kink around 100 meV binding energy in certain regions of k -space is seen [40]. This compound is a charge density wave (CDW) system, and it seems clear that for 2H-TaSe₂ the kink is simply the coupling of the normal band with a back-folded band arising from the CDW (analogous to the shadow bands in Bi2212). This explanation is not expected to apply in other cuprates. A kink in the dispersion also is seen in Sr₂RuO₄ in an orbital-selective manner: a kink occurs at ~25 meV binding energy in the band with d_{xy} character, but not in the bands with d_{xz} , d_{yz} character [41]. A kink was predicted from theory from magnetic fluctuations, [42] *not* for the d_{xy} band but for the other two. There are suggestions that such orbital-specific renormalization could arise from a specific phonon [41] much as has been suggested for Bi2212, [43] but the origin is undecided at this time.

For the cuprates, there are substantial cases for a phonon mechanism [44,45], a polaronic origin (lattice plus strong correlation), [46] for a magnetic fluctuation origin [47,48] of the kink, or less transparently to the resonant mode in the superconducting state [49] or to both phonons and spin fluctuations [50]. This article is not the place to try to explore that issue. Some aspects of the kink are doping dependent, but it is present from under- to over-doping; *i.e.* it is present at optimal doping. One development, from the Dresden group [51], is the argument (independent of origin of the kink) that the ARPES data in the region including the kink can be modeled well with a self-energy expression obtained from the data. They then obtain not only the many-body renormalization, but also the underlying ‘bare’ band structure, which is found to agree with LDA calculations.

5.4. Magnetic fluctuations

The importance of the spin fluctuation spectrum has been recognized since the outset, when HTS were found to evolve from doping of the antiferromagnetic state. The spectrum is strongly doping dependent, with carrier concentration of only $x \approx 0.03$ required to destroy long range magnetic order (see the phase diagram in figure 1). As with other issues discussed here, we note only what the current information in the optimally doped region indicates.

Focus has moved to the extensively studied resonant mode around 40 meV that appears in the superconducting state; T_c of at least 50 K (and presumably the accompanying gap on part of the Fermi surface) is necessary to support this mode. Scattering is only strong in the vicinity of the antiferromagnetic wavevector (π, π) . A recent overview has been provided by Sidis *et al* [52]. The scattering at 40 meV has been seen in Tl2201, in YBCO, and in BSCCO. The mode has a fairly well defined dispersion but only in a small region of the zone near (π, π) ; the actual papers will have to be consulted for details. Both local moment and itinerant magnetism models of the origin of this mode exist, references can be found in, for example, the recent experimental paper of Pailhès *et al.* [53].

In spite of substantial work, new results continue to appear. Recent inelastic neutron scattering on nearly optimally doped YBCO (oxygen content 6.85 rather than 6.92) by Pailhès *et al.* [53]. have uncovered further regions of scattering at 50-60 meV: a commensurate peak at 53 meV that has even symmetry with respect to the two CuO₂ layers (the 40 meV peak has odd symmetry), and diffuse scattering in the 50-60 meV range further from the (π, π) point.

5.5. Phonons

The relevance of phonons in HTS has been addressed much more seriously since it was suggested that the kink in the quasiparticle spectrum observed by ARPES has about the right energy scale and character to result from renormalization due to strong electron-phonon coupling.

(The spin fluctuations discussed above, which have a similar energy scale and are a large-Q excitation, comprise the other main possibility.) As with the other topics in HTS, most of the attention has been paid to the undoped and underdoped region, whereas the focus of this overview is the optimally doped regime.

A recent report on fully oxygenated (optimally doped, $T_c = 93$ K) YBCO detwinned crystals was presented by Pintschovius *et al* [54]. They were able to show (confirming and solidifying earlier reports) that, for Q in both the \hat{a} and \hat{b} directions, the planar-oxygen-derived Cu-O bond stretch modes disperse downward strongly about halfway to the zone boundary, reflecting strong electron coupling to these modes. The softening also shows strong temperature dependence, strengthening as the temperature is lowered. At low T , the mode softens from 67 meV around $Q=0$ to 55 meV at the zone boundary, a relative decrease $\Delta(\omega^2)/\omega_o^2 = 33\%$. In the region of transition between 67 meV and 55 meV the phonon is not a simple phonon-like excitation.

Although there are now several implementations of density functional linear response theory that enables the calculation of phonons of arbitrary wavevector, the many atoms per cell have hampered the application of that method to cuprates so far. The one report is by Savrasov and Andersen [55] on a virtual-crystal-doped version of the infinite layer compound CaCuO_2 , which is structurally the simplest of any cuprate. It is also not representative of hole-doped cuprates, because there is no apical oxygen. Their results for this model compound led to no noticeable phonon anomalies in the oxygen-Cu bond-stretch modes. Possibly this is due to the neglect of any strong correlation on the Cu ion. Of course, it also has to be kept in mind that phonons in the infinite layer material have not been measured, so it is unknown whether the calculated frequencies are correct. The electron-phonon coupling strength they obtained was insufficient to account for an appreciable T_c , however. Several groups have been modeling cuprate phonons, or treating more generic models like the Hubbard-Holstein model where the interplay between strong Cu-site interaction and strong electron-phonon coupling can be studied. Since these models are dealing almost exclusively with the undoped and weakly doped regimes, we will not attempt even a representative citing of the literature in this area.

6. Variations in T_c at optimal doping

Mention was made above that an important outstanding question is: why, in compounds with a given number of CuO_2 layers, the maximum T_c faithfully follows the “rule”: $T_c[\text{Hg}] > T_c[\text{TI}] > T_c[\text{Bi}]$. It is also the case that T_c increases with number n of CuO_2 layers in the cell up to $n=3$, then decreases. More generally one can ask: at optimal doping what material characteristics result in higher T_c ? what changes of parameters increase (or decrease) T_c ? Clearly a broad knowledge of how T_c changes with variation of the crucial parameters, *at fixed*

doping level, should be very important and could be decisive in obtaining a microscopic understanding and theory of HTS. There have been a number of suggestions, mostly related to the suggester’s favored mechanism. It is possible however to approach this question from a simple “material parameter” approach.

6.1. Effect of underlying dispersion relation

The underlying feature of single-band many-body models of HTSs is the dispersion relation for a square lattice in tight-binding form,

$$\begin{aligned} \varepsilon_k = -\sum_R t(\vec{R})e^{i\vec{k}\cdot\vec{R}} = & -2t[\cos(k_x a) + \cos(k_y a)] \\ & -4t'\cos(k_x a)\cos(k_y a) - 2t''[\cos(2k_x a) + \\ & \cos(2k_y a)] + \dots + (\text{interlayer terms}). \end{aligned} \quad (1)$$

Writing this form presumes some *effective Cu $d_{x^2-y^2}$ orbital*, *i.e.* a Wannier function that is orthogonal to identical Wannier functions centered on all other Cu sites. Pavarini *et al.* applied the NMTO band structure method to specify a systematic procedure of constructing such an effective $d_{x^2-y^2}$ -symmetry orbital [56]. For a Bloch sum of these orbitals (a tight-binding-like Bloch sum) they extracted the tight-binding hopping parameters that reproduce the low energy (near Fermi energy) dispersion relation given by LDA.

Their main results were characterized in terms of a range parameter $r \approx |t'/t|$, the ratio of second-to first-neighbor hopping. (The actual definition of r is more intricate, consult the original paper [56] for details.) Their class of materials included around fifteen materials including La-, Y-, Pb-, Tl-, Bi-, and Hg-based members. Two main results emerged. First, for single-layer materials, the resulting value of r varied almost linearly with the apical oxygen height, the value of r being a factor of two higher for the Tl- and Hg-based materials ($T_c^{\text{opt}} \sim 85\text{-}90$ K) than for LSCO ($T_c^{\text{opt}} \sim 45$ K). This relation indicates that second-neighbor hopping involves the apical oxygen height, and the correlation with T_c^{opt} suggests a connection to the mechanism.

Their second result was the establishment of a monotonic increasing (apparently supralinear) trend of T_c^{opt} versus r for these fifteen compounds, which includes one-, two-, and three-layer cuprates. In their method, there is a strong role played by the virtual (unoccupied) Cu 4s orbital, whose energy ε_s is closely connected with the range parameter s . The results of Pavarini *et al.* are not mechanism-specific, but bear directly on the connection of optimal T_c and structure. Markiewicz and collaborators have extended [57] parts of this general line of thinking to take into account the detailed ARPES data that is being accumulated.

6.2. Effect of uniaxial strain on T_c

The pressure experiments mentioned above for the Hg-based two- and three-layer compounds show that, at optimal doping level and ambient pressure, T_c can be

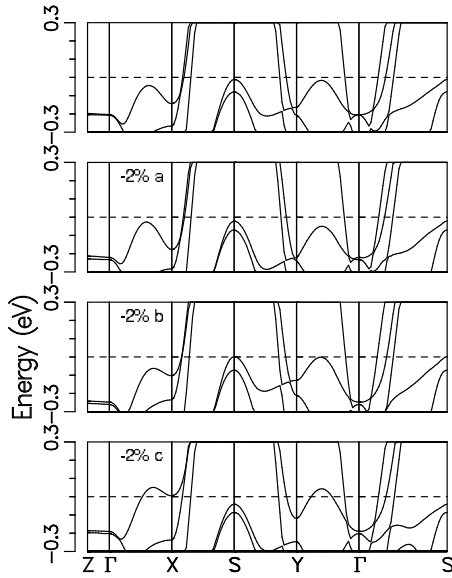


Figure 4. Plots of the band structure within ± 0.3 eV of the Fermi level, for YBCO at equilibrium (top), and for 2% compressive strains along each axis (as marked). Note especially the strong shift in position of the saddle point at the X symmetry point. The band maximum midway between Γ and Y also shifts strongly.

increased (substantially, for Hg1223) by manipulation of internal parameter(s). An important variation on this result had begun to arise even in the early-1990s when the effect of uniaxial strain on T_c in YBCO was established [58-62]. Agreement to within 0.1 K/GPa was obtained, the values being

$$\begin{aligned} dT_c/dp_a &= -2.0K/GPa, \\ dT_c/dp_b &= +2.0K/GPa, \\ dT_c/dp_c &= +0.2K/GPa. \end{aligned} \quad (2)$$

The measured elastic moduli [63] can be used to convert these into strain dependences:

$$\begin{aligned} dT_c/d\varepsilon_a &= +212K, \\ dT_c/d\varepsilon_b &= -244K, \\ dT_c/d\varepsilon_c &= -8K, \end{aligned} \quad (3)$$

with the \hat{c} -axis value being consistent with zero. The rather substantial and opposing values for strains in-plane indicate a surprisingly large effect of the Cu-O chains in the YBCO structure. Sitting at optimal doping, compression along \hat{a} (negative strain) decreases T_c , while compression of the chains (directed along \hat{b}) leads to a surprisingly large enhancement of T_c .

This information no doubt provides important clues into the pairing mechanism. Thinking that it provides a direct means to uncover correlations between changes in various properties of YBCO with the change in T_c , the present author carried out a suite of calculations [64,65] to assemble such correlations. The strain derivatives of properties were calculated using finite differences; it was found that at each strain it was necessary to relax the atomic positions. This involved optimizing five coupled internal parameters, straightforward but tedious. Carrying out these

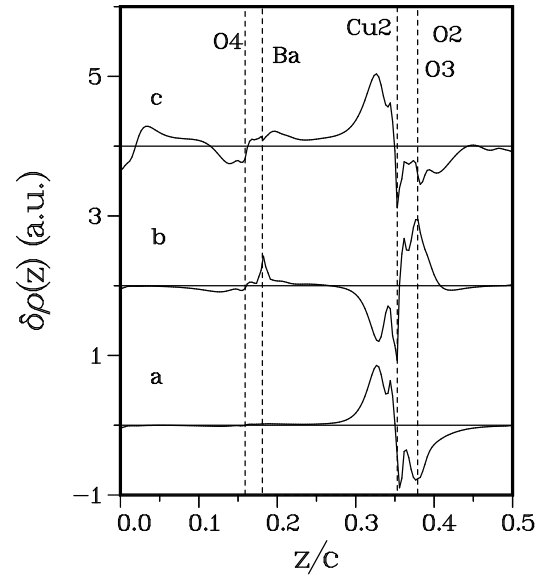


Figure 5. Display of the change in electron charge density, averaged in the $\hat{a}-\hat{b}$ plane, and plotted along the \hat{c} axis, due to 2% strains along the separate axes, as marked. Particularly for the \hat{a} - and \hat{b} -axis strains, the rearrangement is confined to cuprate layer region. Notation: the positions of the atomic layers are denoted by dotted lines, Cu2 is the planar Cu, and O2, O3 denote the oxygen sites in the plane. The apical oxygen is O4, and the Cu-O chain lies at zero on the z/c axis.

calculations had the productive result that the five A_g Raman-active phonon frequencies and their strain dependence resulted.

Analysis gave the uniaxial strain dependence of a number of properties, including: bands near the Fermi level and the various atom- and orbital-projected densities of states; phonon frequencies (and eigenvectors); atomic charges (strictly, the charge within the inscribed spheres) and various layer-averaged charge densities; core levels; Madelung potentials. The significance of these calculational results of course relies on the substantial verification from experiment (phonon frequencies, Fermi surfaces, bare dispersions, etc.) that LDA calculations are reliable for these quantities. The most significant results are those that have opposing sign for \hat{a} - and \hat{b} -axis strains, *i.e.* that correlate with an increase/decrease in T_c , and they include the following:

- i. The \hat{c} -axis internal strain of the planar Cu (*i.e.* its z height) was largest of any, $|dz/d\varepsilon| = 0.008 \text{ \AA}/\%$ and opposite for the two strains.
- ii. The highest frequency (apical oxygen) A_g frequency is unusually sensitive to \hat{b} -axis strain.
- iii. van Hove singularities shift significantly with strains, but no particular correlation of their proximity to the Fermi level to the observed change of T_c could be established. The shifts are presented in the band structures near the Fermi level that are presented in figure 4.
- iiii. Charge rearrangements are dominated by dipolar-like shifts across the CuO_2 layer, as displayed in

figure 5, rather than chain-to-layer shifts that have attracted much more comment in the literature.

This last item appears to settle the charge-transfer question: chain \leftrightarrow plane charge transfer effects are much smaller than intralayer charge rearrangements. But this result raises the intriguing situation: the doping level begins at optimal, and does not change with strain, yet for the correct choice of uniaxial strain (\hat{b} axis for compressive, \hat{a} axis for extension) T_c can be increased substantially. Some parameter(s) of YBCO that strongly affects T_c is sensitive to in-plane strain. There is however no clear identification of a crucial parameter(s) that correlates so strongly with the change in T_c . This direction of research needs more emphasis.

7. Discussion

This overview has been devoted to peeking at the HTS materials and their behavior in a somewhat different way than is conventional. Much, perhaps even most, of the recent work has focused on the underdoped regime where a great deal of complex materials phenomena are occurring, and a lot of this complexity probably has nothing directly to do with the HTS phenomenon. Unfortunately, there is no agreement on what is “interesting” from the HTS viewpoint, and what is peripheral. An important observation here relating to the superconducting state itself is the STM work of Fischer’s group[20]: there are very high T_c (~ 110 K) cuprates for which the superconducting state, as probed by STM spectroscopy, is uniform, one might say spectacularly so.

References

1. T Timusk and B Statt, *Rep. Prog. Phys.* **62** (1999) 61.
2. Y Ando, S Komiyama, K Segawa, S Ono and Y Kurita, *Phys. Rev. Lett.*, **43** (2004) 267001.
3. R H McKenzie, *Science*, **278** (1997) 820.
4. C W Chu, *Nature*, **365** (1993) 323.
5. L Gao, Y Y Xue, F Chen, Q Xiong, R L Meng, D Ramirez, C W Chu, J H Eggert and H K Mao, *Phys. Rev. B* **50** (1994) 4260.
6. C W Chu, L Gao, F Chen, Z J Huang, R L Meng and Y Y Xue, *Nature*, **365** (1993) 323.
7. M Nunez-Regueiro et al., *Science*, **262** (1993) 97.
8. M Muroi and R Street, *Physica C* **208** (1993) 107.
9. A Bianconi, *Solid State Commun.* **84** (1994) 933.
10. A Bianconi, N L Saini, A Lanzara, M Missori, T Rossetti, H Oyanagi, H Yamaguchi, K Oka and T Ito, *Phys. Rev. Lett.* **76** (1996) 3412.
11. J M Tranquada, J D Axe, N Ichikawa, A R Moodenbaugh, Y Nakamura and S Uchida, *Phys. Rev. Lett.* **78** (1997) 338.
12. J Zaanen and O Gunnarsson, *Phys. Rev. B* **40** (1989) R7391.
13. V J Emery, S A Kivelson and H Q Lin, *Physica B* **163** (1990) 306.
14. K Machida, *Physica C* **158** (1989) 192.
15. G Seibold, C Castellani, C Di Castro and M Grilli, *Phys. Rev. B* **58** (1998) 13506.

Thus the inhomogeneity that is so widely studied is not necessarily intrinsic to the optimally doped materials.

In the previous section it was pointed out that one productive avenue for future emphasis is to study more closely the characteristics at optimal doping, and probe what is related sensitively to changes in T_c . Another approach that deserves serious consideration is to look at the theory of HTS coming from the overdoped side. The initial state is apparently a reasonably standard Fermi liquid, then as the carrier concentration in the CuO_2 layer(s) is reduced HTS asserts itself, before being torn apart by the encroachment of strong antiferromagnetic fluctuations and other correlation effects (and in the underdoped regime inhomogeneity may in fact be intrinsic). Approached from this direction, conventional (perturbative, diagrammatic) many-body theory may be applicable all the way to optimal doping.

Acknowledgments

I have benefitted from discussion and collaboration with numerous workers in the field. I acknowledge specific recent communications with J. Fink, O. Fischer, and B. Keimer. Z.-X. Shen is acknowledged for figure 3 of LSCO ARPES data. Our recent work in this area has been supported by National Science Foundation Grant DMR-0421810. Support from the Alexander von Humboldt Foundation, and the hospitality of IFW Dresden, during the preparation of this manuscript is gratefully acknowledged.

16. Z Islam, X Liu, S K Sinha, J C Lang, S C Moss, D Haskel, G Srajer, P Wochner, D R Lee, D R Haeffner and U Welp, *Phys. Rev. Lett.* **93** (2004) 157008.
17. I Martin, D Podolsky and S A Kivelson, *Phys. Rev. B* **72** (2005) 060502.
18. K Aryanpour, E R Dagotto, M Mayr, T Paiva, W E Pickett and R T Scalettar, *Phys. Rev. B* **73** (2006) 104518.
19. K McElroy, D-H Lee, J E Hoffman, K M Lang, J. Lee, E W Hudson, H Eisaki, S Uchida and J C Davis, *Phys. Rev. Lett.* **94** (2005) 197005.
20. M Kugler, D Lde Castro, E Giannini, A Piriou, A A Manuel, C Hess and O Fischer, *J. Phys. Chem. Solids* **67** (2006) 353.
21. M Braden, M Meven, W Reichardt, L Pintschovius, M T Fernandez-Diaz, G Heger, F Nakamura and T Fujita, *Phys. Rev. B* **63** (2001) 140510.
22. A Damascelli, Z Hussain and Z-X Shen, *Rev. Mod. Phys.* **75** (2003) 473.
23. J C Campuzano, M R Norman and M Randeria, in *Physics of Conventional and Unconventional Superconductors*, Vol. 2, edited by K. H. Bennemann and J B Ketterson (Springer-Verlag, Berlin, 2004).
24. W E Pickett, R E Cohen, H Krakauer and D J Singh, *Science*, **255** (1992) 46.
25. W E Pickett, R E Cohen and H Krakauer, *Phys. Rev.*

- Lett.* **67** (1991) 228.
26. W E Pickett, *Rev. Mod. Phys.* **61** (1989) 433.
 27. X J Zhou, T Yoshida, S A Kellar, P V Bogdanov, E D Lu, A Lanzara, M Nakamura, T Noda, T Kakeshita, H Eisaki, S Uchida, A Fujimori, Z Hussain and Z-X Shen, *Phys. Rev. Lett.* **86** (2001) 5578.
 28. A Ino, C Kim, M Nakamura, T Yoshida, T Mizokawa, A Fujimori, Z-X Shen, T Kakeshita, H Eisaki and S Uchida, *Phys. Rev. B* **65**(2002) 094504.
 29. P B Allen, W E Pickett and H Krakauer, *Phys. Rev. B* **36** (1987) 3926.
 30. P B Allen, W E Pickett and H Krakauer, *Phys. Rev. B* **37** (1988) 7482.
 31. H Krakauer and W E Pickett, *Phys. Rev. Lett.* **60** (1988) 1665.
 32. P Aebi, J Osterwalder, P Schwaller, L Schlapbach, M Shimoda, T Mochiku and K Kadowaki, *Phys. Rev. Lett.* **72** (1994) 2757.
 33. H Ding, A F Bellman, J C Campuzano, M Randeria, M R Norman, T Yokoya, T Takahashi, H Katayama-Yoshida, T Mochiku, K Kadowaki, G Jennings and G P Brivio, *Phys. Rev. Lett.* **76** (1996) 1533.
 34. M C Schabel, C-H Park, A Matura, Z-X Shen, D A Bonn, R Liang and W N Hardy, *Phys. Rev. B* **57** (1998) 6107 and references therein.
 35. O K Andersen, A I Liechtenstein, O Rodriguez, I I Mazin, O Jepsen, V P Antropov, O Gunnarsson and S Gopalan, *Physica C* **185-189** (1991) 147.
 36. O K Andersen, O Jepsen, A I Liechtenstein and I I Mazin, *Phys. Rev. B* **49** (1994) 4145.
 37. D H Lu, D L Feng, N P Armitage, K M Shen, A Damascelli, C Kim, F Ronning, Z-X Shen, D A Bonn, R Liang, W N Hardy, A I Rykov and S Tajima, *Phys. Rev. Lett.* **86** (2001) 4370.
 38. P V Bogdanov, A Lanzara, S A Kellar, X J Zhou, E D Lu, W J Zheng, G Gu, J-I Shimoyama, K Kishio, H Ikeda, R Yoshizaki, Z Hussain and Z X Shen, *Phys. Rev. Lett.* **85** (2000) 2581.
 39. A Lanzara, P V Bogdanov, X J Zhou, S A Kellar, D L Feng, E D Lu, T Yoshida, H Eisaki, A Fujimori, K Kishio, J-I Shimoyama, T Noda, S Uchida, Z Hussain and Z-X Shen, *Nature*, **412** (2001) 510-514.
 40. K Rossnagel, E Rotenberg, H Koh, N V Smith and L Kipp, *Phys. Rev. B* **72** (2005) 121103.
 41. H Iwasawa, Y Aiura, T Saitoh, I Hase, S I Ikeda, Y Yoshida, H Bando, M Higashiguchi, Y Miura, X Y Cui, K Shimada, H Namatame, and M Taniguchi, *Phys. Rev. B* **72** (2005) 104514.
 42. D Manske, I Eremin and K H Bennemann, *Phys. Rev. B* **67** (2003) 134520.
 43. T P Devereaux, T Cuk, Z-X Shen, and N Nagaosa, *Phys. Rev. Lett.* **93** (2004) 117004.
 44. F J Ohkawa, *Phys. Rev. B* **70** (2004) 184514.
 45. R Citro, S Cojocaru and M Marinaro, *Phys. Rev. B* **73** (2006) 014527.
 46. W Koller, A C Hewson, and D M Edwards, *Phys. Rev. Lett.* **95** (2005) 256401.
 47. M Randeria, A Paramekanti, and N Trivedi, *Phys. Rev. B* **69** (2004) 144509.
 48. A V Chubukov and M R Norman, *Phys. Rev. B* **70** (2004) 174505.
 49. P D Johnson, T Valla, A V Fedorov, Z Yusof, B O Wells, Q Li, A R Moodenbaugh, G D Gu, N Koshizuka, C Kendziora, S Jian, and D G Hinks, *Phys. Rev. Lett.* **87** (2001) 177007.
 50. J-X. Li, T Zhou and Z D Wang, *Phys. Rev. B* **72** (2005) 094515.
 51. A A Kordyuk, S V Borisenko, A Koitsch, J Fink, M Knupfer and H Berger, *Phys. Rev. B* **71** (2005) 214513.
 52. Y Sidis, S Pailhès, B Keimer, P Bourges, C Ulrich, L P Regnault, *Phys. Stat. Sol. B* **241** (1994) 1204.
 53. S Pailhès, Y Sidis, P Bourges, V Hinkov, A Ivanov, C Ulrich, L P Regnault and B Keimer, *Phys. Rev. Lett.* **93** (2004) 167001.
 54. L Pintschovius, D Reznik, W Reichardt, Y Endoh, H Hiraka, J M Tranquada, H Uchiyama, T Masui, and S Tajima, *Phys. Rev. B* **69** (2004) 214506.
 55. S Y Savrasov and O K Andersen, *Phys. Rev. Lett.* **77** (1996) 4430-4433.
 56. E Pavarini, I Dasgupta, T Saha-Dasgupta, O Jepsen, and O K Andersen, *Phys. Rev. Lett.* **87** (2001) 047003.
 57. R S Markiewicz, S Sahrakorpi, M Lindroos, H Lin, and A Bansil, *Phys. Rev. B* **72** (2005) 1054519.
 58. C Meingast, O Kraut, T Wolf, and H Wühl, A Erb and G Müller-Vogt, *Phys. Rev. Lett.* **67** (1991) 1634.
 59. O Kraut, C Meingast, G Brauchle, H Laus, A Erb, G Müller-Vogt and H. Wühl, *Physica C* **205** (1993) 139.
 60. C Meingast, J Karpinski, E Jilek, and E Kaldis, *Physica C* **209** (1993) 139.
 61. U Welp, M Grimsditch, S Fleshler, W Nessler, J Downey, G W Crabtree, and J Guimpel, *Phys. Rev. Lett.* **69** (1992) 2130.
 62. U Welp, M Grimsditch, S Fleshler, W Nessler, B Veal, and G W Crabtree, *J. Supercond.* **7** (1994) 159.
 63. M Lei, *Phys. Rev. B* **47** (1993) 6154.
 64. W E Pickett, *Physica C* **289** (1997) 51.
 65. W E Pickett, *Phys. Rev. Lett.* **78** (1997) 1960.